

Tests of Hypercubic Fermion Actions

T. DeGrand

Physics Department, University of Colorado,
Boulder, CO 80309 USA

(the MILC collaboration)

Abstract

I have performed scaling tests using quenched spectroscopy of a family of fermion actions which have a hypercubic kinetic term, gauge connections built of smeared links, and an anomalous magnetic moment term. These actions show improved rotational invariance compared to the standard Wilson action and to the tadpole-improved clover action. Hyperfine splittings are improved compared to the standard Wilson action (at the level of a factor of three in the lattice spacing), and are about the same as for the tadpole-improved clover action.

1 Introduction

I report on tests of a family of fermion actions for lattice gauge theory simulations, which are designed to improve scaling of hadron spectroscopy. While very expensive to simulate, they appear to more than repay their computational cost with better scaling behavior.

The actions which I tested were inspired by the fixed point (FP) action program [1, 2] for fermions[3, 4, 5, 6, 7, 8, 9, 10]. However, they are not FP actions. They are Wilson-fermion like, in the sense that they have four component spinors on all sites and there are no manifest symmetries which protect the bare quark mass from being additively renormalized.

The new features which I tested include:

1) a hypercubic kinetic energy term. Each fermion in the action communicates with $3^4 - 1 = 80$ nearest neighbors. This term improves the hadron dispersion relation compared to that from actions using a standard on-axis nearest neighbor coupling.

2) Gauge connections built of very fat gauge links, links built by averaging the fundamental link variables over a local region and re-projecting them back onto the gauge group. This construction removes short distance fluctuations from the correlators during the simulation process, rather than attempting to divide them out at the end. This results in observed very small additive mass renormalization of bare quantities, and I conjecture that all perturbative corrections to observables are considerably reduced. To include very fat links in a simulation with dynamical fermions using known technology might be quite expensive, but in quenched simulations the cost is minimal.

I also tested a complicated lattice anomalous magnetic momentum term in which the quark and antiquark are not fixed to the same site. Some kind of term is needed to correct the lattice free quark magnetic moment and to improve meson and baryon hyperfine splittings. However, my tests show that the standard “clover” term, suitably normalized, improves scaling as much as the complicated Pauli term needed to satisfy the FP equations.

The scaling tests in this paper are a bit non-standard (when compared to other studies of spectroscopy) and deserve some explanation. I am interested in scaling tests which are uncontaminated by extrapolations in volume or to the chiral limit. Thus I compare only simulations in fixed physical volume. Any volume would do, and so I choose a small one simply because these actions are expensive to simulate. To set the scale I use a gluonic observable because

these are quenched simulations. As a choice of gluonic observables, one has T_c , the critical temperature for deconfinement, the string tension σ or the Sommer radius r_0 . Glueball or torelon measurements are just too costly. Of these observables, the ones associated with the potential (σ and r_0) require a fit to a function $V(r)$; the choice of the fitting function can affect the results. At very coarse lattice spacing this problem becomes more serious. Thus I use T_c to set the scale, and do simulations on lattices of fixed size $L = 2/T_c$. With $\sqrt{\sigma} \simeq 440$ MeV and $\sqrt{\sigma}/T_c \simeq 1.60$, the scales are $T_c = 275$ MeV, $L = 1.45$ fm, and $2\pi/L = 860$ MeV. Lattice spacings $aT_c = 1/2, 1/3, 1/4$ correspond to $a = 0.36, 0.24$, and 0.18 fm.

All the tests are performed at fixed physical quark mass (defined either by interpolating lattice data to a fixed value of m_π/m_ρ or to a fixed value of m_π/T_c). At very coarse lattice spacing, and with heavy (though still relativistic) quarks, scaling violations from conventional actions are very large. Thus only modest statistics are required to identify improvement—or lack thereof—compared to them.

Besides spectroscopy, I measure the meson or baryon dispersion relation. In lattices of fixed physical volume set by T_c , the physical momenta corresponding to the different allowed lattice modes are multiples of T_c , $a\vec{p} = 2\pi\vec{n}/L$ or $\vec{p} = \pi T_c \vec{n}$, if $L = 2/T_c$, and one can compare data with different lattice spacings at the same physical momentum. Wilson and clover fermions at $\beta < 6.0$ (using the Wilson gauge action) exhibit bad scaling or rotational invariance violations. The new actions are rotationally invariant even at $a = 0.36$ fm.

The outline of the paper is as follows: In Section 2 I describe the new features of these actions. Section 3 is devoted to scaling tests, and I make some tentative conclusions in Section 4. I describe the (new) FP gauge action used in these simulations in the Appendix.

2 Ingredients of the Actions

2.1 Hypercubic kinetic term

The fermionic free field action has the generic form

$$\Delta_0(x) = \lambda(x) + i \sum_{\mu} \gamma_{\mu} \rho_{\mu}(x). \quad (1)$$

It is constructed by finding some free FP action [3, 4, 5, 6]. We begin with a continuum action for fermions which has no doublers and is chirally symmetric. We construct an action on a coarser distance scale Δ' by iterating the FP equation

$$\begin{aligned}
(\Delta')_{n_b, n'_b}^{-1} &= \frac{1}{\kappa} \delta_{n_b, n'_b} \\
&+ \Omega_{n_b, n}(\Delta)_{n, n'}^{-1} \Omega_{n', n'_b}^T
\end{aligned}
\tag{2}$$

where Ω is a blocking kernel and κ is a tunable parameter. We select a blocking kernel, iterate the RGT to find a fixed point action, and then tune parameters in Ω to make the action maximally local. We have used a factor-of-two rescaling in which Ω is restricted to a hypercube: Ω_{ij} is nonzero only if $j = i \pm \mu$, $i \pm \mu \pm \nu$, \dots , $i \pm \mu \pm \nu \pm \lambda \pm \sigma$, and $\Omega_{ij} = c((i-j)_1, (i-j)_2, (i-j)_3, (i-j)_4)$. Each site communicates to $3^4 - 1 = 80$ neighbors.

There are many good parameterizations, resulting in fairly local FP actions. However, one ultimately wants to use these actions in simulations, and the action must be somehow truncated. There are a number of (subjective) criteria to select a good RGT, based on the properties of the truncated action (which the RGT does not know about): a good dispersion relation, $E(p) = |\vec{p}|$ out to large $|\vec{p}|$ with no complex roots, good free-field thermodynamics, $P = 1/3\sigma T^4$ even at large discretization, etc. We tuned the RGT to optimize these criteria, and our choice is given by $c(1, 0, 0, 0) = 0.03$, $c(1, 1, 0, 0) = 0.01$, $c(1, 1, 1, 0) = 0.005$, $c(1, 1, 1, 1) = 0.0025$, and $\kappa = 44.0$.

The couplings of the FP action for our RGT (for massless fermions) fall off exponentially with $r = \sqrt{\sum_{\mu} x_{\mu}^2}$. The largest entries at distance $r = 2$ are at location $x = (\pm 1, \pm 1, \pm 1, \pm 1)$. The smallest truncation which accurately reproduces the main features of this FP action is to an action which sits on a hypercube—that is, the free field action is to be parameterized with five nonzero λ 's and four nonzero ρ 's, corresponding to each of the nonzero offsets. An example of a dispersion relation for this hypercubic action is compared to the Wilson action in Figs. 1 and 2. We show both branches of the hypercubic action's dispersion relation; all roots are real. The non-truncated FP action has a perfect dispersion relation $E = |\vec{p}|$ for all \vec{p} .

For massive fermions, we need an action which is on a renormalized trajectory (RT) for some RGT (with the mass scaling at each step with the ratio of lattice spacings). To reach the RT, one can begin with an action which has a very small mass but is otherwise close to a FP action, perform a series of blockings, and follow it out.

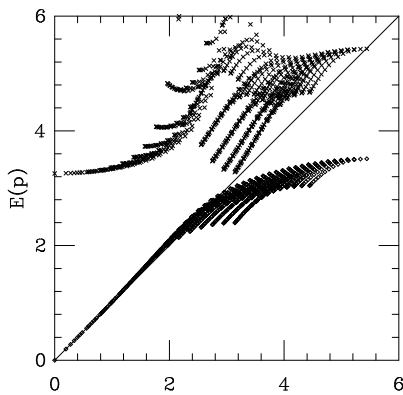


Figure 1: Dispersion relation $E(p)$ vs $|p|$ for $m_0 = 0$ for the hypercubic action.

One complication with this procedure is that an action which is local for small mass can block into an action for large mass which is not short range. To avoid this, I take an RG transformation whose parameters are functions of the mass and tune the parameter(s) to insure a local action at each blocking step. The resulting λ 's and ρ 's are smooth functions of the mass. Again, the dispersion relation for hypercubic approximations to RT actions are well behaved out to large $|\vec{p}|$.

Plots of the variation of the parameters—or the tables of numbers corresponding to them—are by themselves not very useful for calculation. Rather than give them, I will immediately present a simple parameterization of the couplings.

My choice of parameterization is to regard all the ρ 's and λ 's as linear functions of the bare mass and to determine $\lambda(0, 0, 0, 0)$ for positive bare mass by solving the dispersion relation for it: defining

$$R = 2\rho_0(1, 0, 0, 0) + 12\rho_0(1, 1, 0, 0) + 24\rho_0(1, 1, 1, 0) + 16\rho_0(1, 1, 1, 1) \quad (3)$$

$$A_s = 2\lambda(1, 0, 0, 0) + 12\lambda(1, 1, 0, 0) + 24\lambda(1, 1, 1, 0) + 16\lambda(1, 1, 1, 1) \quad (4)$$

$$D = 8\lambda(1, 0, 0, 0) + 24\lambda(1, 1, 0, 0) + 32\lambda(1, 1, 1, 0) + 16\lambda(1, 1, 1, 1) \quad (5)$$

the pole of the propagator ($\lambda^2(p) + \sum_{\mu} \rho_{\mu}^2(p) = 0$ at $p_{\mu} = (im_0, 0, 0, 0)$) is at

$$\lambda(0, 0, 0, 0) = -A_s \cosh(m_0 - 1) - R \sinh(m_0) - D. \quad (6)$$

My linear parameterization runs over $0 < m_0 < 0.32$, which is the useful range of mass for light hadron spectroscopy for lattice spacings $aT_c = 1/2$ to $1/4$.

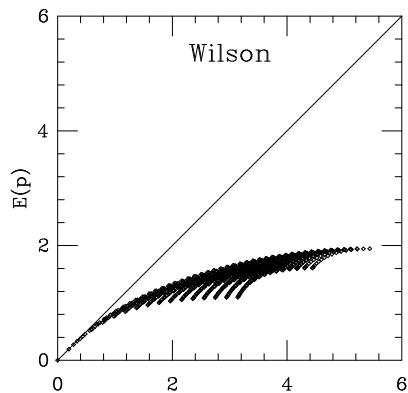


Figure 2: Dispersion relation $E(p)$ vs $|p|$ for massless Wilson fermions.

The big problem in parameterizing an approximate action is that the additive renormalization of the quark mass for $g^2 \neq 0$ drives the critical quark mass m_q^c negative, outside the region where the solution of the FP equation is meaningful. With Wilson fermions, and one free parameter (κ) this is not a problem (one just tunes κ above κ_c without otherwise altering the action) but with these complicated actions there is not a clear cut way to proceed. In principle, all the parameters in the action should depend on properties of the gauge field (for example, on the local value of the plaquette). To circumvent this, I make an arbitrary choice: I assume that the parameters continue to vary linearly with the bare mass, and I determine $\lambda(0, 0, 0, 0)$ by continuing the low-mass limit of Eqn. 6 to negative mass.

$$\lambda(0, 0, 0, 0) = -A_s - D - Rm_0. \quad (7)$$

Since $m_q^c \simeq -0.4$ at $\beta_c(N_t = 4)$ and moves toward zero at bigger β 's, $\lambda(0, 0, 0, 0)$ is basically a linear function of m_0 .

This parameterization is not appropriate for studying charm with this action (where $am_0 = 2$ to 4 depending on the lattice spacing). The parameters of the action on the RT are smooth functions of m_0 , so one could probably construct a more complicated (polynomial or exponential) fit to them.

Table 1 gives the parameters of the linear fit.

Table 1: Linear parameterization of the couplings of the hypercubic action:
 $\lambda(x_0, x_1, x_2, x_3) = \lambda_a + m_0 \lambda_b$, $\rho_0(x_0, x_1, x_2, x_3) = \rho_a + m_0 \rho_b$.

offset	λ_a	λ_b	ρ_a	ρ_b
0 0 0 0	2.256756	-0.9863		
1 0 0 0	-0.1122	0.0741	-0.1464	0.1300
1 1 0 0	-0.0323	0.0271	-0.0329	0.0303
1 1 1 0	-0.0144	0.0141	-0.0101	0.0096
1 1 1 1	-0.0072	0.0076	-0.0035	0.0033

2.2 Very Fat Links

Measurements of pure gauge observables (the potential or glueball masses) suffer from noise arising from the short distance fluctuations of the gauge fields. A good cure for this problem has been known for many years: define new link variables which do not couple to the UV sector of the lattice variables, and which have the same IR properties as the original variables. An example of such a variable is an APE-blocked link [11]

$$\begin{aligned}
 V_\mu^{n+1}(x) = & (1 - \alpha)V_\mu^n(x) + \alpha/6 \sum_{\nu \neq \mu} (V_\nu^n(x)V_\mu^n(x + \hat{\nu})V_\mu^n(x + \hat{\nu})^\dagger \\
 & + V_\nu^n(x - \hat{\nu})^\dagger V_\mu^n(x - \hat{\nu})V_\mu^n(x - \hat{\nu} + \hat{\mu})) \quad (8)
 \end{aligned}$$

(with $V_\mu^0(x) = U_\mu(x)$ and $V_\mu^{n+1}(x)$ is projected back onto $SU(3)$). It is also known that for best results, both α and the maximum number of blocking steps N should increase as the lattice spacing decreases.

Fermions also suffer from bad UV behavior, and their symptoms include the breaking of flavor symmetry (for staggered fermions), large additive renormalization of the bare mass (for Wilson fermions), and large renormalizations of currents (for any kind of fermion). The tadpole improvement program [12] was originally designed to estimate or compute these large UV effects and subtract (or divide) them out during the conversion from the lattice calculation to continuum number.

However, recent evidence suggests that it may in some cases be better to remove the UV fluctuations directly from the simulations. This evidence is the partial restoration of flavor symmetry breaking for staggered fermions by replacing the link by an $N = 1$ APE-blocked link, as shown by Ref. [13] and (with a slightly different averaging) by Ref. [14]. These authors restrict themselves to $N = 1$, presumably because they wish to use their actions for simulations with dynamical fermions. However, if one is interested in quenched simulations, one can APE-block to any desired level, with tiny overhead, simply by pre-

computing and storing the APE-blocked links. Then if $N > 1$ improves UV behavior, one is free to use it.

It is easy to understand why the fat links suppress UV fluctuations [15]. Each term in the action in coordinate space

$$\mathcal{L}_I = \frac{1}{2a} \sum_{x,y,z} \bar{\psi}(x) \Gamma \dots U_\mu(x+y) \dots \psi(x+z) \quad (9)$$

can be expanded as a power series in g

$$\begin{aligned} \mathcal{L}_I = & \frac{1}{2a} \sum_{x,y,z} \bar{\psi}(x) \Gamma \dots (1 + i g a A_\mu(x+y+a/2\hat{\mu}) \\ & - \frac{1}{2} (a g)^2 A_\mu(x+y+a/2\hat{\mu})^2 \dots) \dots \psi(x+z) \end{aligned} \quad (10)$$

which in momentum space becomes $\mathcal{L}_I = \mathcal{L}_I^1 + \mathcal{L}_I^2$ with

$$\mathcal{L}_I^1 = i \frac{g}{2} \int_{p,q} \bar{\psi}(p) \Gamma \int_k \delta^4(k+q-p) A_\mu(k) e^{i(y+a/2\hat{\mu})k} \psi(q) e^{iqz} \quad (11)$$

$$\begin{aligned} \mathcal{L}_I^2 = & \frac{g^2 a}{2} \int_{p,q} \bar{\psi}(p) \Gamma \int_{k_1,k_2} \delta^4(k_1+k_2+q-p) A_\mu(k_1) A_\mu(k_2) \\ & e^{i(y+a/2\hat{\mu})(k_1+k_2)} \psi(q) e^{iqz}. \end{aligned} \quad (12)$$

Smearing the link over a distance r_0 makes the replacement

$$A_\mu(r + \frac{a}{2}\hat{\mu}) \rightarrow \sum_{\mu,\nu} \sum_w h_{\mu\nu}(w) A_\nu(r+w + \frac{a}{2}\hat{\nu}) \quad (13)$$

or

$$A_\mu(k) \rightarrow \sum_{\mu,\nu} H_{\mu\nu}(k) A_\nu(k) e^{i(y+a/2(\hat{\nu}-\hat{\mu}))k} \quad (14)$$

(and a similar formula for \mathcal{L}_I^2) where the form factor is $H_{\mu\nu}(k) = \sum_r h_{\mu\nu}(r) e^{ikr}$. Essentially any smearing function suppresses the vertex at $k > \pi/r_0$. In the language of Ref. [12], tadpoles contribute beyond their naive strength because the UV divergence of the gluon loop compensates for the a -dependence of the vertex; smearing suppresses the coupling of the fermion to high momentum gluons.

2.3 Nonlocal Pauli Term

Lattice fermions have a magnetic moment which is anomalously small due to lattice artifacts. One can parameterize the vertex through the interaction of a

fermion with an infinitesimal magnetic field B : the pole in the propagator will be at $E = m_0 + B/2m_B$, where m_B is the so-called magnetic mass. We write the momentum-space interaction term as

$$\bar{\psi}(p)i\Delta_\mu^1(p, -p')A_\mu(p - p')\psi(p') \quad (15)$$

and expand the vertex in Dirac space as

$$\begin{aligned} \Delta_\mu^1(k, -p) = & f_{\mu,0}(k, -p) + f_{\mu,\nu}(k, -p)\gamma_\nu + \sum_{\rho < \nu} f_{\mu,\rho\nu}(k, -p)\gamma_\rho\gamma_\nu \\ & + f_{\mu,5}(k, -p)\gamma_5 + f_{\mu,\nu 5}(k, -p)\gamma_\nu\gamma_5 \end{aligned} \quad (16)$$

(with an identical labeling for the decomposition in coordinate space). A lot of algebra [5] gives

$$m_B = -\frac{\lambda(im_0)[\lambda'(im_0) - \rho'_0(im_0)]}{\rho'_2(im_0)f_{1,1}(im_0) - ic_{12}^1(im_0)\lambda(im_0)} \quad (17)$$

where

$$\lambda(im) = \sum_n e^{mn_0} \lambda(n) \quad (18)$$

$$\lambda'(im) = \sum_n n_0 e^{mn_0} \lambda(n) \quad (19)$$

$$\rho'_0(im) = -i \sum_n n_0 e^{mn_0} \rho_0(n) \quad (20)$$

$$\rho'_2(im) = -i \sum_n n_2 e^{mn_0} \rho_2(n) \quad (21)$$

$$f_{1,1}(im) = \sum_{xy} e^{mx} f_{1,1}(x, y) \quad (22)$$

$$ic_{12}^1(im) = \sum_{xy} (x - 2y)_2 e^{mx} f_{1,12}(x, y) \quad (23)$$

are all real.

All approximate FP vertices I have seen have a complicated Pauli term with sizable contributions when the quark and antiquark do not sit on the same lattice site. As an example, Table 2 shows the contribution of various fermion offsets to $ic_{12}^1(x, im)$ for a vertex based on the RGT we have been using in this paper. The normalization appears to be reasonably well saturated by fermion offsets over a cube. The gauge connections are very complicated.

However, it is not clear how important the FP version of the Pauli term will be in spectroscopy. I therefore studied three possibilities:

x	$m_0 = 0.08$	$m_0 = 0.16$	$m_0 = 0.32$	$m_0 = 0.64$
0 0 0 0	-0.0913	-0.0840	-0.0709	-0.0527
1 0 0 0	-0.2490	-0.2269	-0.1883	-0.1278
1 1 0 0	-0.2980	-0.2710	-0.2253	-0.1479
1 1 1 0	-0.1641	-0.1493	-0.1248	-0.0816
1 1 1 1	-0.0318	-0.0291	-0.0246	-0.0167
Sum in hypercube:	-0.8343	-0.7604	-0.6340	-0.4269
Total:	-0.8974	-0.8182	-0.6837	-0.4807

Table 2: Nonlocality of the Pauli term $ic_{12}^1(x, im)$ for actions along the RT.

1) No Pauli term at all. This turns out to give hyperfine interactions which are too small.

2) Keep only the on-site part of the Pauli term (the standard clover term) but choose its normalization so that $m_B = m_0$. This is not a FP action. The gauge links will be fattened like the rest of the links in the action.

3) Restrict the Pauli term to offsets which span a cube. For each offset, sum over all the minimum-length paths (with their sign factors) which contribute to the Pauli term. Choose the relative normalization of the terms to match the FP vertex and the overall normalization to fix $m_B = m_0$. Fatten the links if necessary. This choice (hereafter called a “full Pauli action”) is a much better approximation to a FP action than the second choice (“clover action”), but if the clover action performs as well in a test, it is the action of choice.

For $m_0 > 0$ the constraint $m_B = m_0$ fixes the normalization of the Pauli term. I find that the normalization varies roughly linearly with the bare quark mass. I choose (arbitrarily) to keep the same linear dependence with m_0 even for negative bare mass. This would be equivalent in the standard clover action, to making the size of the clover term a function of the hopping parameter κ , rather than a function of β . From a practical point of view the difference is slight: as one varies the gauge coupling in a simulation, the value of bare quark corresponding to a particular physical hadron mass shifts, becoming (typically) more negative as β decreases. The input coefficient of the clover term becomes larger as β decreases, so the net result is that one can as well say that the clover term tracks the bare quark mass, as to say that the it tracks the bare coupling. At zero gauge coupling FP actions do not have a mass-independent Pauli normalization and so the standard practice of making the normalization mass independent is unnatural. Presumably one could do simulations with a standard action, such as the Wilson-plus-clover action, tuning m_B to equal m_0 , although it is hard to see the point of doing this as long as the dispersion relation is imperfect.

The linear parameterization reproduces $m_B = m_0$ to within five per cent for $m_0 < 0.4$. For the clover hypercubic action I could have simply set $m_B = m_0$ for $m_0 > 0$ by inverting Eqn. 17, although I did not do that.

3 Scaling Tests

3.1 Survey of Actions Tested

Most of the quenched spectroscopy has been done using a new parameterization of a FP gauge action for SU(3). In the Appendix I tabulate the critical temperature, string tension, and Sommer parameters for the gluonic action, so the reader can convert to his favorite scaling variable. One test has been done using the original parameterization of the action presented in Ref. [16], and some tests use the SU(3) gauge action of our recent work on instantons[17]. We have made rough measurements of its $\beta_c(N_t)$ for deconfinement to set the scale.

All the fermionic actions are made gauge-invariant by replacing the offsets by an average over the shortest distance gauge paths. For example,

$$\bar{\psi}(x)\psi(x + \hat{\mu} + \hat{\nu}) \rightarrow \frac{1}{2}\bar{\psi}(x)[V_\mu(x)V_\nu(x + \hat{\nu}) + V_\nu(x)V_\mu(x + \hat{\mu})]\psi(x + \hat{\mu} + \hat{\nu}) \quad (24)$$

where $V_\mu(x)$ is either one of the original links or an APE-blocked link.

The cost of a hypercubic action per iteration step during matrix inversion is about 20 times as expensive as the usual Wilson action, since there are more neighbors and the Dirac connections are not projectors. Actions with the complicated Pauli term are about 56 times as expensive as the usual Wilson action. All the gauge connections are pre-computed, so there are startup and storage costs, as well. I used the stabilized biconjugate gradient (biCGstab) algorithm for matrix inversion [18].

The two actions which were tested most extensively both have a hypercubic kinetic term and APE-blocked links with $N = 7$ and $\alpha = 0.3$. Action A has a full Pauli term. It is the best approximation to a FP action I found. It used the very expensive gauge action of Ref. [17]. Action C has only the clover term but is otherwise identical. My scaling tests of it used the new gauge action presented in the Appendix.

I tested several other actions. All the variants of tadpole improvement I studied had large mass renormalization. A pure hypercube action with no Pauli

term had a good dispersion relation at the coarsest lattice spacing, but its hyperfine splittings were basically identical to those of the Wilson action.

3.2 Spectroscopy

Lattice volumes were $4^3 \times 16$ at $aT_c = 1/2$ (excessively long in the time direction, in retrospect), $6^3 \times 16$ at $aT_c = 1/3$, and $8^3 \times 16$ (dangerously short) and $8^3 \times 24$ (safer) at $aT_c = 1/4$.

The data set for Action A consists of 80 lattices at $aT_c = 1/2$, 50 lattices at $aT_c = 1/3$ and 36 $8^3 \times 16$ lattices at $aT_c = 1/4$. The data set for Action C consists of 80 lattices at $aT_c = 1/2$ and $aT_c = 1/3$ and 60 $8^3 \times 24$ lattices at $aT_c = 1/4$.

The spectroscopy measurement is entirely straightforward. I gauge fixed to Coulomb gauge and used a Gaussian independent particle source wave function $\psi(r) = \exp(-\gamma r^2)$ with $\gamma = 1, 0.5, \text{ and } 0.25$ at $aT_c = 2, 3, 4$. I used pointlike sinks projected onto low momentum states. I used naive currents ($\bar{\psi}\gamma_5\psi$, etc.) for interpolating fields. The spectra appeared to be asymptotic (as shown by good (correlated) fits to a single exponential) beginning at $t \simeq 2$ (at $aT_c = 1/2$), 3-5 (at $aT_c = 1/3$) and 5-7 (at $aT_c = 1/4$) and the best fits were selected using the old HEMCGC criterion [19].

My fiducial for comparison, simply because there are extensive data sets, is Wilson-action quenched spectroscopy. I have tried to restrict the data I used for comparison to lattices with the proper physical volume. I constructed my own $aT_c = 1/2$ and $aT_c = 1/3$ Wilson data sets ($\beta = 5.1$ and 5.54) since I could not find any results for these. I also ran off 40 Wilson lattices at $\beta = 5.7$ ($N_t = 4$) to measure a dispersion relation. At that coupling my masses were within a standard deviation of the much superior data set of Butler, et al. [20].

To compare with the more standard improved actions, I also performed a fiducial study using the clover action (Wilson fermion action plus on-site clover term) in a background of Wilson action gauge fields. I tadpole-improved the action using $u_0 = (\text{Tr}U_p/3)^{1/4}$ where U_p is the average plaquette. Data are at $aT_c = 1/2$ and $aT_c = 1/3$, where $u_0 = 0.802$ and 0.844 . This data set was 180 and 60 lattices at the two couplings.

I show first plots of m_ρ/T_c and m_N/T_c vs. m_π/T_c with Wilson fermions. These plots are scaling tests by themselves, or one can interpolate in the curves to fixed values of m_π/T_c (equivalent to fixed quark mass) and plot the variation in the observable vs. aT_c . Fig. 3 shows the rho mass and Figs. 4 shows the

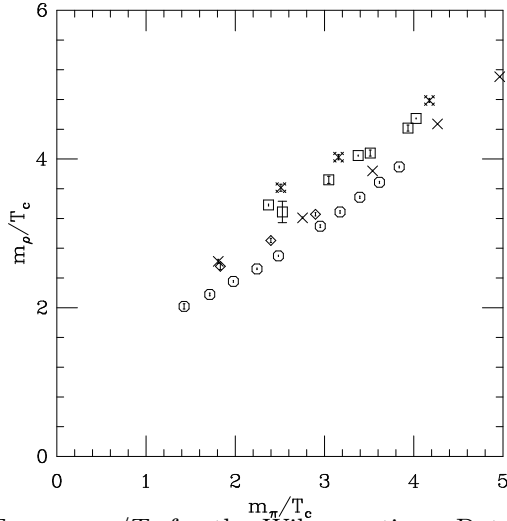


Figure 3: m_ρ/T_c vs. m_π/T_c for the Wilson action. Data are labelled with octagons for $aT_c = 1/2$, diamonds for $aT_c = 1/3$, crosses for $aT_c = 1/4$, squares for $aT_c = 1/8$, and fancy crosses for $aT_c = 1, 12$.

nucleon mass. Notice that the rho mass has the worst scaling violations of the three particles.

We can roughly estimate the critical bare quark mass (at which the pion is massless) by linearly extrapolating m_π^2 to zero in m_0 . Fig. 5 shows the squared pion mass vs bare quark mass for action A, at β_c for $N_t = 2, 3, 4$, and the same plot, but for action C, is shown in Fig. 6. Both actions have small bare mass renormalization. This is important from the point of view of principle because a true FP action would have no additive mass renormalization. It is important in practice because we only really know the kinetic parameters by solving the RG equation for positive bare mass; they must be extrapolated in some artistic way if one needs to go to negative bare mass.

Another way to estimate the critical bare mass is to use or the PCAC relation

$$\nabla_\mu \cdot \langle \bar{\psi} \gamma_5 \psi(0) \bar{\psi} \gamma_5 \gamma_\mu \psi(x) \rangle = 2m_q \langle \bar{\psi} \gamma_5 \psi(0) \bar{\psi} \gamma_5 \psi(x) \rangle. \quad (25)$$

If we convert to lattice operators, sum over spatial slices, and measure distance in the t direction, this becomes:

$$Z_A \frac{\partial}{\partial t} \sum_{x,y,z} \langle \bar{\psi} \gamma_5 \psi(0) \bar{\psi} \gamma_5 \gamma_0 \psi(x) \rangle = 2am_q Z_P \sum_{x,y,z} \langle \bar{\psi} \gamma_5 \psi(0) \bar{\psi} \gamma_5 \psi(x) \rangle. \quad (26)$$

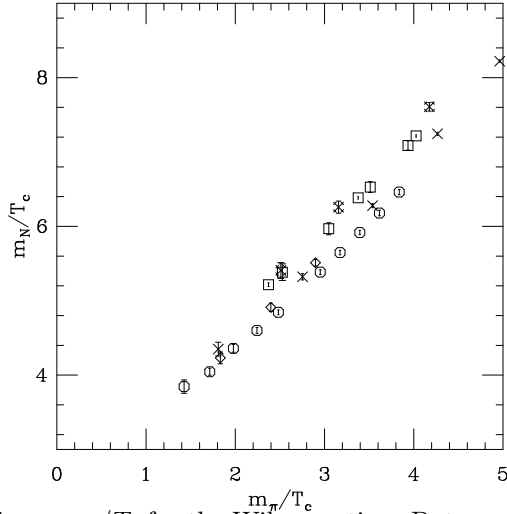


Figure 4: m_N/T_c vs. m_π/T_c for the Wilson action. Data are labelled as in Fig. 11.

I follow [21] by fitting the pseudoscalar source-pseudoscalar sink to

$$P(t) = Z(\exp(-m_\pi t) + \exp(-m_\pi(N_t - t))) \quad (27)$$

and the pseudoscalar source-axial sink to

$$A(t) = \frac{Z_P}{Z_A} \frac{2m_q}{m_\pi} Z(\exp(-m_\pi t) - \exp(-m_\pi(N_t - t))). \quad (28)$$

to extract m_q . There are many other possibilities for defining an axial current and for defining the derivative operator. I only use the naive (pointlike) currents. I do not know the Z -factors, but for finding the value of m_0^c that does not matter. Extrapolating m_π^2 or m_q linearly in m_0 ignores all the well-known problems associated with extracting quark masses from lattice data [22], but the procedure is perfectly adequate to distinguish a small quark mass from a large one. The quark masses are shown in Figs. 5 and 6.

We find for action A that $m_0^c = -0.42, -0.20,$ and -0.14 at $aT_c = 1/2, 1/3,$ and $1/4,$ respectively. For action C, the corresponding numbers are $m_0^c = -0.36, -0.16,$ and -0.095 . These numbers should be compared to the analogous quantities for Wilson fermions, using $m_0^c = 1/(2\kappa_c) - 4$: -1.58 at $\beta = 5.1$ ($aT_c = 1/2$), -1.04 at $\beta = 5.7$ ($aT_c = 4$), and still -0.70 at $\beta = 6.3$ [12]. In the latter case tadpole improved perturbation theory can explain most of the mass shift.

Now for scaling tests. I compare m_ρ/T_c and m_N/T_c vs. m_π/T_c for actions

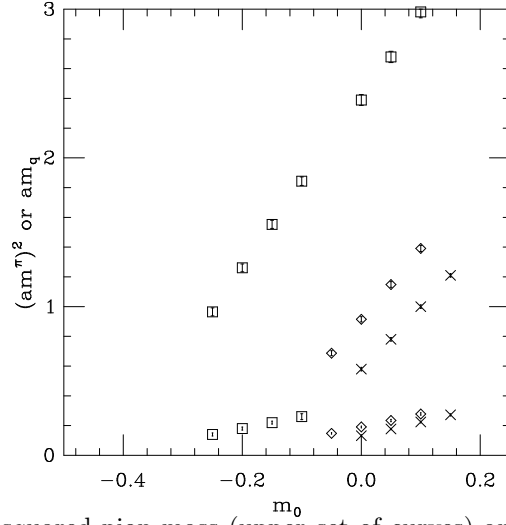


Figure 5: Bare squared pion mass (upper set of curves) and quark mass from Eq. 40 (lower set of curves) vs bare quark mass for action A, at β_c for $N_t = 2$ (squares), 3 (diamonds), 4 (crosses).

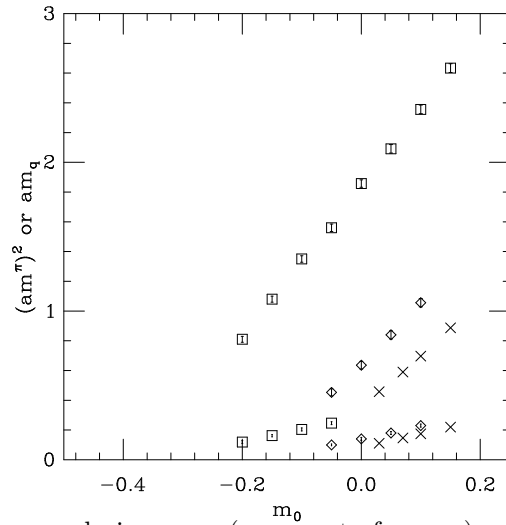


Figure 6: Bare squared pion mass (upper set of curves) and quark mass from Eq. 40 (lower set of curves) vs bare quark mass for action C, at β_c for $N_t = 2$ (squares), 3 (diamonds), 4 (crosses).

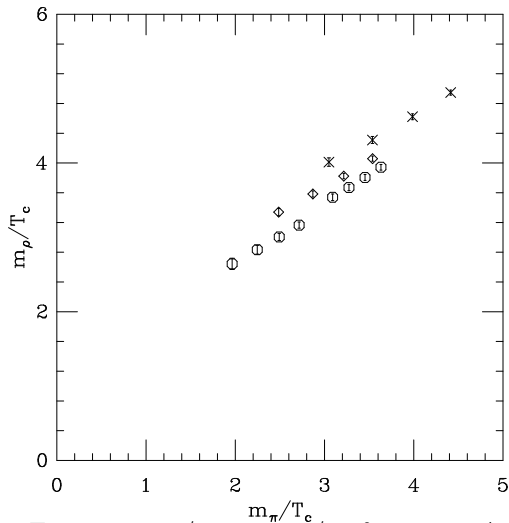


Figure 7: m_ρ/T_c vs. m_π/T_c for action A.

A and C in Figs. 7, 8, 9, and 10.

We can compare scaling violations in hyperfine splittings by interpolating our data to fixed π/ρ mass ratios and plotting the N/ρ mass ratio vs. $m_\rho a$. I do this at four π/ρ mass ratios, 0.80 and 0.70, in Fig. 11. In these figure the diamonds are Wilson action data in lattices of fixed physical size (4^3 at $\beta = 5.1$, 6^3 at $\beta = 5.54$, 8^3 at $\beta = 5.7$ [20], 16^3 at $\beta = 6.0$ [23] 24^3 at $\beta = 6.3$ [24]) and the crosses are data in various larger lattices: 16^3 and 24^3 at $\beta = 5.7$ and 32^3 at $\beta = 6.17$ [20], 24^3 at $\beta = 6.0$ [23]. When they are present the data points from larger lattices illustrate the danger of performing scaling tests with data from different volumes. The bursts are from the nonperturbatively improved clover action of Ref. [25] and the fancy diamonds are the TI clover action. The other plotting symbols show our test actions A and C.

We give a tables of masses from Action C in Tables 3, 4, and 5, and for Action A in Tables 6, 7, and 8.

3.3 Dispersion Relations

There are two ways to look at dispersion relations. The simplest is to plot $E(p)$ the energy of the state produced with spatial momentum \vec{p} , as a function of $|\vec{p}|$. The result for action C at bare mass 0.15 is compared to the free dispersion relation at $aT_c = 1/2$ in Fig. 12. All of the test actions I have studied have

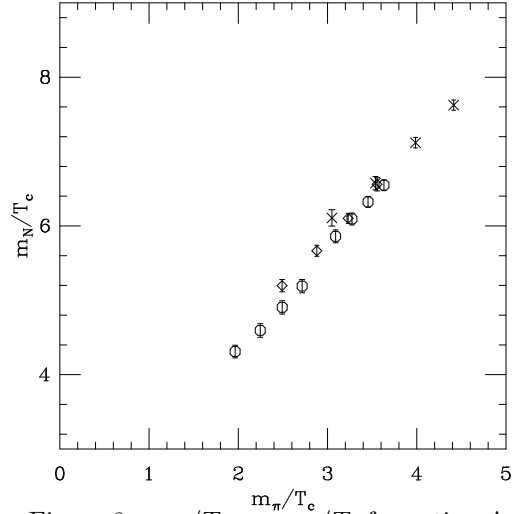


Figure 8: m_N/T_c vs. m_π/T_c for action A.

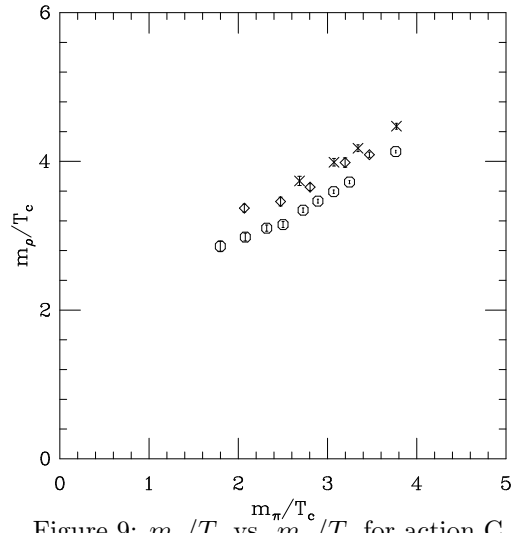


Figure 9: m_ρ/T_c vs. m_π/T_c for action C.

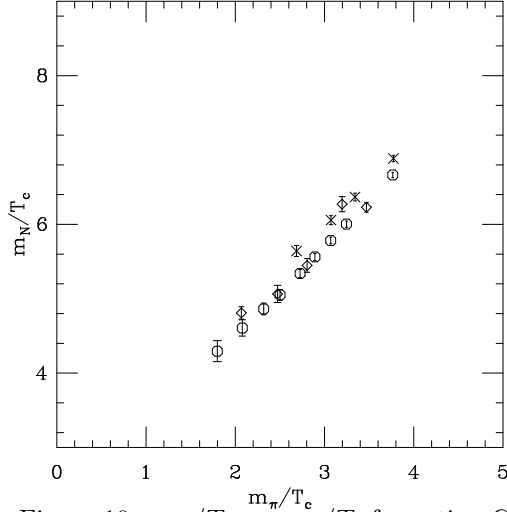


Figure 10: m_N/T_c vs. m_π/T_c for action C.

good dispersion relations even at $aT_c = 1/2$. I believe that is a generic feature of the hypercubic kinetic term.

The signal to noise ratio for the nonzero momentum meson channels dies away at large t like $\exp(-(E(p) - m_\pi)t)$. This means that large statistics are required to go to small quark mass or to high \vec{p} . However, it is possible to extract a fitted $c_{eff}^2 = (E(p)^2 - m^2)/p^2$ for the lowest nonzero momentum mode, for larger masses. This was done by performing a 4-parameter correlated fit to a pair of single exponentials, one for the $\vec{p} = (0,0,0)$ mode and the other the $\vec{p} = (1,0,0)$ mode. I compare my results from action C and from the Wilson and clover actions in Figs. 13 and 14. Hadron masses are again scaled by T_c to allow the display of several lattice spacings at once. Action C has $c_{eff}^2 \simeq 1$ for all observed hadrons even at $p = \pi T_c$ (860 MeV/c) at $aT_c = 1/2$.

3.4 Summary

It appears that these actions are members of a family of actions which show improved scaling, even at $\beta_c(N_t = 2)$, about 0.36 fm lattice spacing.

The hypercubic actions have much better dispersion relations than either the clover or Wilson action. They share this improvement with the D234 family of actions [26] and with the Hamber-Wu [27] action as tested in Ref. [28].

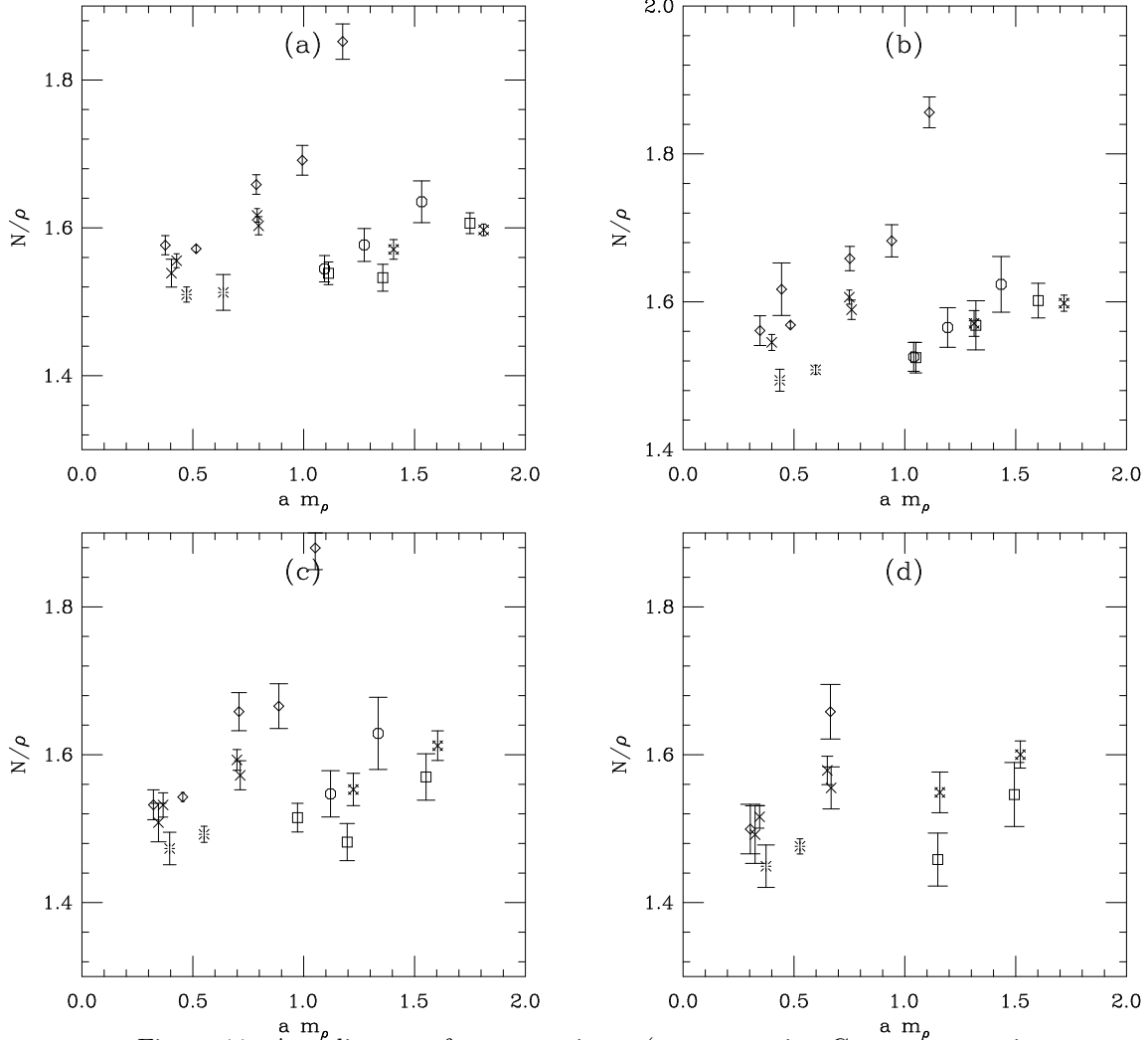


Figure 11: A scaling test for new actions: (squares action C, octagons action A) vs. Wilson actions on lattices of fixed physical size (diamonds) and larger volumes (crosses), and the nonperturbatively improved (bursts) and tadpole improved (fancy crosses) clover actions. Data are interpolated to $\pi/\rho = 0.84$ (a), 0.80 (b), 0.75 (c) and 0.70 (d).

am_q	PS	V	N	Δ
0.30	1.883(8)	2.066(8)	3.332(17)	3.450(21)
0.15	1.623(9)	1.861(10)	3.002(20)	3.156(25)
0.10	1.535(9)	1.796(11)	2.891(22)	3.061(27)
0.05	1.446(9)	1.733(12)	2.781(24)	2.967(30)
0.00	1.363(9)	1.672(14)	2.670(27)	2.875(33)
-0.05	1.251(10)	1.575(20)	2.526(37)	2.770(46)
-0.10	1.159(10)	1.551(20)	2.432(39)	2.687(43)
-0.15	1.039(12)	1.491(26)	2.303(54)	2.591(49)
-0.20	0.899(16)	1.429(35)	2.147(70)	2.505(64)

Table 3: Table of best-fit masses, action C, $\beta = 3.092$ ($aT_c = 1/2$).

am_q	PS	V	N	Δ
0.15	1.156(7)	1.363(11)	2.077(21)	2.258(28)
0.10	1.066(15)	1.328(20)	2.090(33)	2.277(51)
0.05	0.935(8)	1.218(15)	1.816(30)	2.049(31)
0.00	0.825(9)	1.153(19)	1.688(38)	1.959(41)
-0.05	0.689(10)	1.124(18)	1.603(27)	1.941(33)

Table 4: Table of best-fit masses, action C, $\beta = 3.50$ ($aT_c = 1/3$).

am_q	PS	V	N	Δ
0.15	0.943(4)	1.118(9)	1.722(10)	1.853(14)
0.10	0.836(4)	1.044(11)	1.592(12)	1.742(17)
0.07	0.768(5)	0.997(12)	1.514(14)	1.678(19)
0.03	0.672(5)	0.934(15)	1.410(18)	1.598(22)

Table 5: Table of best-fit masses, action C, $\beta = 3.70$ ($aT_c = 1/4$).

am_q	PS	V	N	Δ
0.15	1.816(11)	1.972(18)	3.274(36)	3.355(44)
0.10	1.727(11)	1.903(19)	3.161(37)	3.309(49)
0.05	1.637(11)	1.835(21)	3.047(39)	3.237(47)
0.00	1.546(11)	1.769(22)	2.930(43)	3.156(51)
-0.10	1.358(10)	1.582(20)	2.596(44)	2.825(43)
-0.15	1.246(10)	1.502(24)	2.452(44)	2.718(49)
-0.20	1.123(11)	1.417(29)	2.297(45)	2.605(57)
-0.25	0.982(13)	1.322(37)	2.155(42)	2.483(71)

Table 6: Table of best-fit masses, action A, $\beta = 2.38$ ($aT_c = 1/2$).

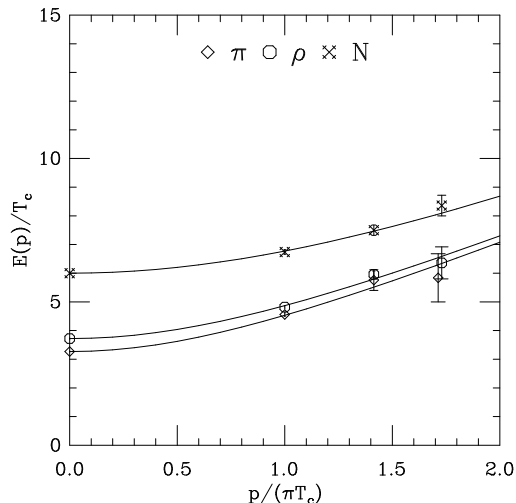


Figure 12: Dispersion relation for heavy hadrons at $aT_c = 1/2$ ($a \simeq 0.36$ fm) from action C. The curves are the continuum dispersion relation for the appropriate (measured) hadron mass.

am_q	PS	V	N	Δ
0.10	1.179(8)	1.353(11)	2.145(19)	2.245(24)
0.05	1.072(8)	1.275(12)	2.010(21)	2.115(27)
0.00	0.956(9)	1.194(13)	1.870(24)	1.989(32)
-0.05	0.829(10)	1.113(16)	1.720(28)	1.854(40)

Table 7: Table of best-fit masses, action A, $\beta = 2.85$ ($aT_c = 1/3$).

However, the hypercubic actions tested here seem to produce about the same level of improvement in hyperfine splittings as the clover action, at heavier quark masses. Leaving out the Pauli term gives noticeable scaling violations with a too-large N/ρ ratio; probably one needs to keep some kind of explicit Pauli/clover term in the lattice action to boost the hyperfine splittings.

The hyperfine splittings show worse scaling violations than the dispersion relation. Controlling and approximating the quark anomalous magnetic moment is the most difficult part of the construction of a FP action, and that may be the source of the scale violations.

Of course, there is still the possibility that all the actions tested here are missing some other common physics ingredient, which is responsible for scaling of the hyperfine splittings.

Since the ρ meson is the particle which shows the largest scaling violations,

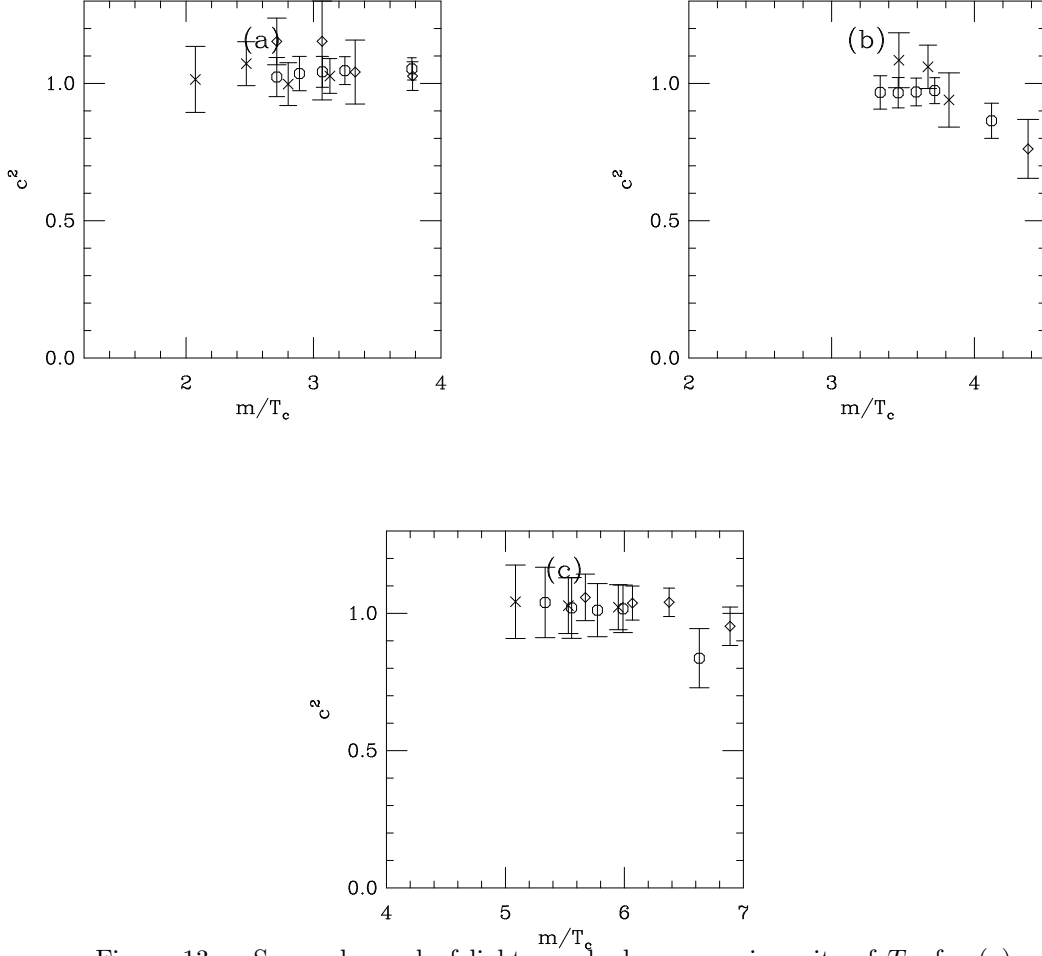


Figure 13: Squared speed of light vs. hadron mass in units of T_c , for (a) pseudoscalars, (b) vectors) and (c) protons, from action C. Octagons, crosses, and diamonds label $aT_c = 1/2, 1/3$ and $1/4$.

am_q	PS	V	N	Δ
0.15	1.100(5)	1.228(8)	1.903(20)	1.998(27)
0.10	0.993(6)	1.146(9)	1.783(18)	1.875(30)
0.05	0.880(6)	1.066(11)	1.640(20)	1.788(26)
0.00	0.758(7)	1.000(12)	1.504(25)	1.662(29)

Table 8: Table of best-fit masses, action A, $\beta = 3.05$ ($aT_c = 1/4$).

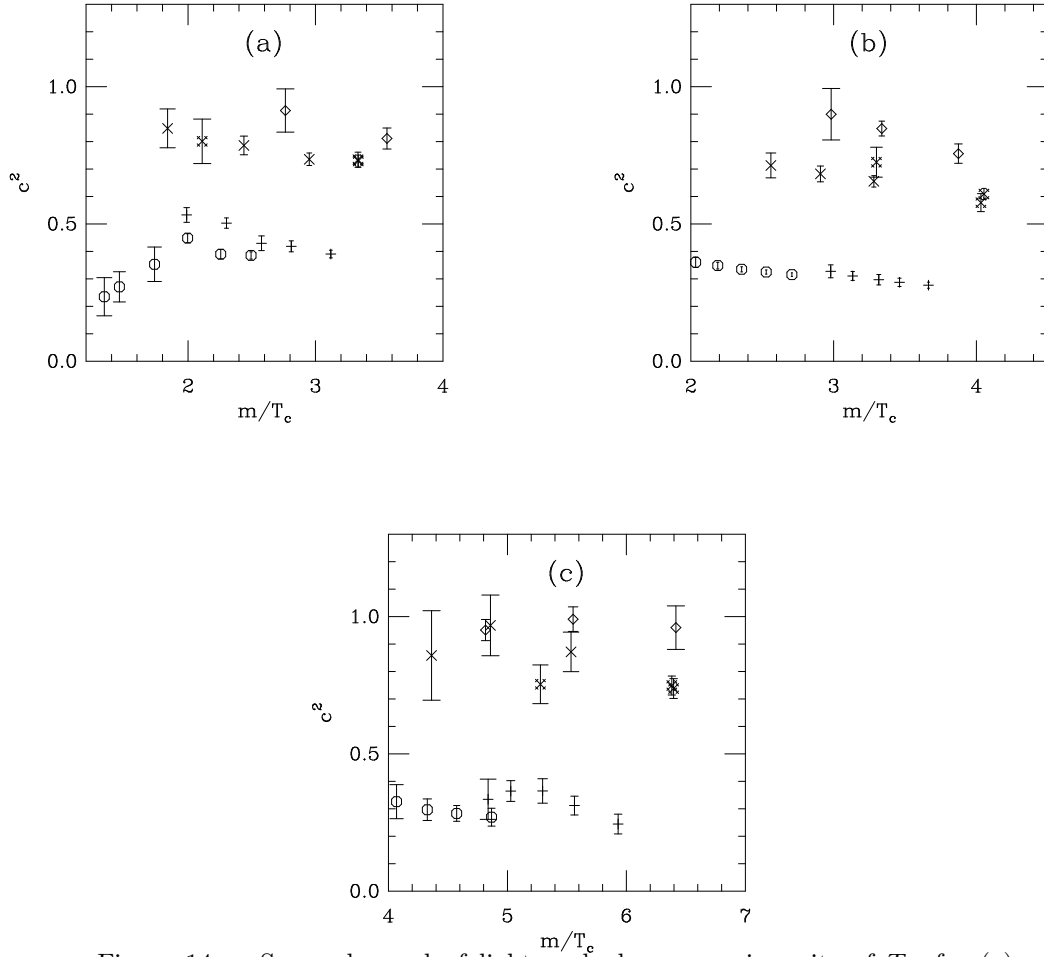


Figure 14: Squared speed of light vs hadron mass in units of T_c , for (a) pseudoscalars, (b) vectors) and (c) protons, from the Wilson and clover actions. Octagons, crosses, and diamonds label $aT_c = 1/2$, $1/3$ and $1/4$ for the Wilson action, and for the clover action the labels are pluses for $aT_c = 1/4$ and fancy crosses for $aT_c = 1/3$.

the best way to quantify improvement is by taking “sections” of the m_ρ/T_c and m_N/T_c vs. m_π/T_c plots and displaying them vs. aT_c at fixed m_π/T_c in Fig. 15. The improved actions at $aT_c = 1/2$ seem to show the same level of scaling violations as Wilson data at a lattice spacing a factor of 3 smaller. The smaller lattice spacing data seem to pick up about a factor of two improvement in lattice spacing, although the uncertainty in the data is larger. Quenched calculations are thought to scale in difficulty like $1/a^6$; the cost of action C is about a factor of 20 compared to the Wilson action.

My data by themselves do not suggest a unique way to extrapolate to $a = 0$. FP actions are classically perfect with no a^n scaling violations for any n . Approximate FP actions generally have discretization errors at all orders in a , though the coefficients of any order in a are typically much smaller than the corresponding coefficient in an a^N improved action (for $n > N$).

4 Conclusions

The important ingredients of these actions which contribute to their improved scaling behavior are the hypercubic kinetic term and the lattice anomalous magnetic moment term. The very small additive renormalization of the bare lattice mass is due to the use of fermion- gauge field couplings which are insensitive to the short-distance fluctuations of the gauge fields.

The specific implementation of these ideas in the actions I have tested involves many arbitrary choices. I believe that essentially every choice I made for a particular parameterization could be replaced by another choice, which would give an action which would have the same quality of scaling violations. Some changes should add some additional good feature. For example, it might be possible to find a parameterization of a fat link which would lend itself to simple perturbation theory calculations.

There are several obvious extensions of this work. The first involves the kinetic term: It would be useful to find a parameterization of the kinetic term which extends from zero mass to very large mass. It would also be interesting to develop a fat link parameterization of the action which could be efficiently incorporated into one of the standard algorithms for dynamical fermions. Next, is there a better parameterization of the anomalous magnetic moment term which might improve scaling?

Fixed point actions have many desirable formal properties [10]: they include scale invariant instanton solutions, the index theorem, an absence of exceptional

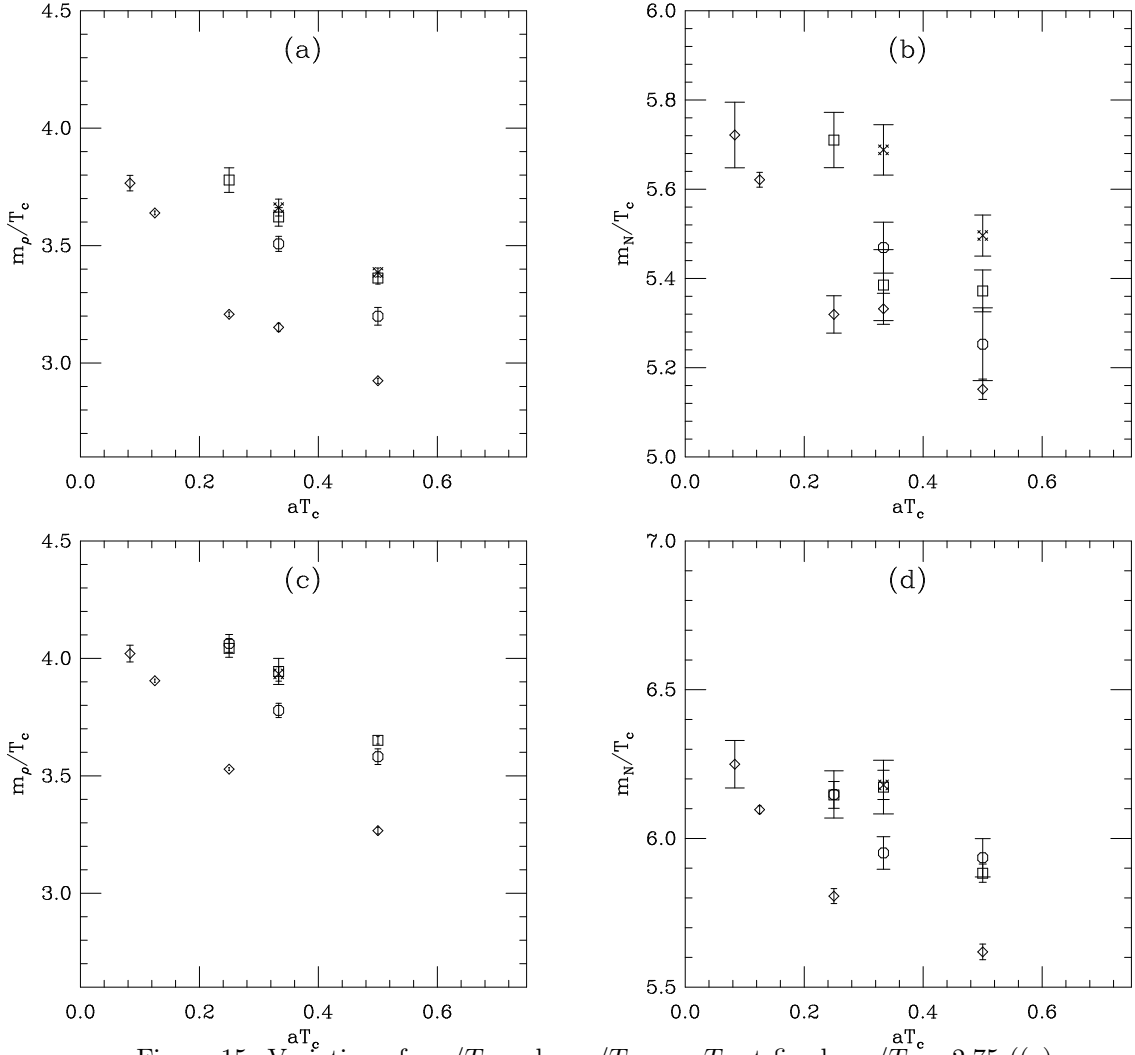


Figure 15: Variation of m_ρ/T_c and m_N/T_c vs. aT_c at fixed $m_\pi/T_c = 2.75$ ((a) and (b)) and 3.15 ((c) and (d)), for actions A (octagons), C (squares), Wilson action (diamonds), and TI clover action (fancy crosses).

configurations, and a remnant of chiral symmetry [29, 30]. These properties may not be present in an action which is a bad approximation to a FP action. I do not know how well they are satisfied by these actions (other than the apparent small renormalization of the quark mass.)

Indeed, the particular choice of a free field action which I made was motivated only by the locality and spectral properties of the free action. No attempt was made to optimize the chiral properties of the approximate action. This is clearly the outstanding problem for future study.

A Pure Gauge Actions

This work used a new few-parameter approximation to an FP action for $SU(3)$ gauge theory. Using it, isolated instanton configurations have constant actions to within 1.5 per cent. Like the action of Ref. [16], it is a superposition of powers of the plaquette and the perimeter-6 “twisted” link $(x, y, z, -x, -y, -z)$. Like the action of Ref. [17] it includes a constant term. It is designed to be used for couplings such that the lattice spacing is $aT_c \simeq 1/3$ or $1/4$ to $1/8$ or so. Explicitly

$$S(V) = c_0 + \frac{1}{N_c} \sum_C (c_1(C)(N_c - \text{Tr}(V_C)) + c_2(C)(N_c - \text{Tr}(V_C))^2 + \dots \quad (\text{A.1})$$

with coefficients tabulated in Table 9.

Table 9: Couplings of the few-parameter approximate FP action.

operator	c_1	c_2	c_3	c_4	$c_0 = -2.517$
c_{plaq}	3.248	-1.580	.1257	.0576	
$c_{6\text{-link}}$	-.2810	.0051	.00490	-.0096	

This action costs about a factor of 7 times the usual Wilson plaquette action to simulate.

I have measured the critical couplings for the deconfinement transition at $aT_c = 1/2, 1/3,$ and $1/4$. The critical couplings on the measured spatial volumes and my extrapolation to infinite volume are shown in Table 10. I have also measured the string tension from Wilson loops at these values of the coupling, on 8^4 lattices (at $\beta = 3.092$) and 12^4 lattices for the other couplings. The data was fitted to a static potential $V(r)$ of the form

$$V(r) = V_0 + \sigma r - E/r \quad (\text{A.2})$$

using the techniques of Ref. [31]. The fit to the largest lattice spacing data is very difficult. The signal from large r is not good, and there is very little left of the Coulomb part of the potential due to the coarseness of the lattice. Nevertheless, I present the string tension and the Sommer [32] parameter r_0 ($r_0^2 dV(r_0)/dr = -1.65$) in Table 10. We see scaling within errors for both these parameters (vs. T_c) at $aT_c = 1/3$ and $1/4$. There is a ten per cent scaling violation at $aT_c = 1/2$. The asymptotic value inferred from large scale Wilson simulations [33] is $\sqrt{\sigma}/T_c = 1.600(11)$.

Finally, I show a plot of $V(r)/T_c$ vs rT_c for the three lattice spacings in Fig. 16. The overall vertical shift in the potentials is not physical, but it allows the reader to separate the different data sets by eye.

Table 10: Critical couplings at finite volume and extrapolated to infinite volume for the FP action with parameters in Table 1.

volume	$N_t = 2$	$N_t = 3$	$N_t = 4$
4^3	3.025(25)		
6^3	3.06(1)	3.47(1)	
8^3	3.08(1)	3.49(1)	3.67(1)
10^3	3.085(5)	3.50(1)	3.69(1)
12^3			3.69(1)
infinite	3.092(7)	3.50(1)	3.70(1)
T_c/Λ	8.67	8.96	8.33
$a^2\sigma$	0.56(5)	.302(16)	.164(3)
$\sqrt{\sigma}/T_c$	1.50(7)	1.65(2)	1.62(2)
r_0/a	1.3(2)	2.19(2)	2.93(1)
r_0T_c	.65(10)	.730(7)	.733(3)

Acknowledgements

This work is an outgrowth of an ongoing project with A. Hasenfratz, P. Hasenfratz, and F. Niedermayer to construct true FP actions for four-dimensional fermions. I am indebted to them for many discussions about this work. I would also like to thank R. Brower, and U. Wiese for valuable conversations about FP actions, and S. Gottlieb, U. Heller, R. Sugar and D. Toussaint for advice on supercomputing. I would like to thank the Colorado high energy experimental groups for allowing me to use their work stations. This work was supported by the U.S. Department of Energy, with some computations done on the T3E at Pittsburgh Supercomputing Center through resources awarded to the MILC collaboration.

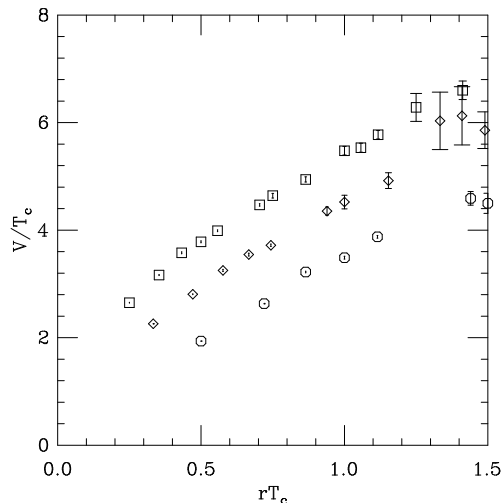


Figure 16: The potential of the approximate FP action, vs distance, scaled with T_c . Octagons show data for $aT_c = 1/2$, diamonds for $aT_c = 1/3$, and squares for $aT_c = 1/4$.

References

- [1] P. Hasenfratz and F. Niedermayer, Nucl. Phys. B414 (1994) 785.
- [2] T. DeGrand, A. Hasenfratz, P. Hasenfratz, F. Niedermayer, Nucl. Phys. B454 (1995) 587; Nucl. Phys. B454 (1995) 615.
- [3] U. J. Wiese, Phys. Lett. B315 (1993) 417.
- [4] W. Bietenholz and U. J. Wiese, Nucl. Phys. B464 (1996) 319.
- [5] T. DeGrand, A. Hasenfratz, P. Hasenfratz, P. Kunszt, F. Niedermayer, Nucl. Phys. B (Proc. Suppl.) 53, 1997, 938, and ongoing work.
- [6] W. Bietenholz, et al., Nucl. Phys. B(Proc. Suppl.) 53 (1997) 921.
- [7] K. Originos, et al., contribution to Lattice '97, hep-lat/9709100.
- [8] C. B. Lang and T. K. Pany, hep-lat/9707024.
- [9] F. Farchioni and V. Laliena, talk presented at Lattice '97, hep-lat/9709040.
- [10] Cf. the review by P. Hasenfratz at Lattice '97, hep-lat/9709110.
- [11] M. Falcioni, M. Paciello, G. Parisi, B. Taglienti, Nucl. Phys. B251[FS13], 624 (1985). M. Albanese, et. al. Phys. Lett. B192, 163 (1987).

- [12] G. Parisi, in the Proceedings of the XX International Conference on High Energy Physics, L. Durand and L. Pondrom, eds., American Institute of Physics, p. 1531. G. P. LePage and P. Mackenzie, Phys. Rev. **D48** (1993) 2250.
- [13] T. Blum, et al., Phys. Rev. **D55**, 1133 (1997).
- [14] J.-F. Lagaë and D. K. Sinclair, talk presented at Lattice '97, hep-lat/9709035.
- [15] For a similar explanation, see G. P. Lepage, Lectures at the 1996 Schlading Winter School, hep-lat/9607076. See the exercise containing Eqs. 78 and 79.
- [16] T. DeGrand, A. Hasenfratz, P. Hasenfratz, F. Niedermayer, Nucl. Phys. **B454** (1995) 615.
- [17] T. DeGrand, A. Hasenfratz, T. Kovacs, hep-lat/9705009.
- [18] For a review of matrix inversion algorithms, see A. Frommer, Nucl. Phys. B (Proc. Suppl.) 53 (1997) 120.
- [19] K. M. Bitar, et al., Phys. Rev. **D42** (1990) 3794.
- [20] F. Butler, H. Chen, J. Sexton, A. Vaccarino, and D. Weingarten, Nucl. Phys. **B430** (1994) 179.
- [21] C. Bernard, et al., Phys. Rev. **D45** (1992) 3854.
- [22] Cf. R. Gupta and T. Bhattacharya, Phys. Rev. **D55** (1997) 7203.
- [23] M. Gockeler, et al. Phys. Lett. **B391** (1997) 388.
- [24] M. Guagnelli, et al., Nucl. Phys. **B378** (1992) 616.
- [25] M. Göckeler, et. al., hep-lat/9707021.
- [26] M. Alford, T. R. Klassen and G. P. Lepage, talk at Lattice '97, hep-lat/9709126 and hep-lat/9712005.
- [27] H. Hamber and C. M. Wu, Phys. Lett. B133 (1983) 351; B136 (1984) 255.
- [28] F. X. Lee and D. Leinweber, hep-lat/9711044
- [29] P. Ginsparg and K. Wilson, Phys. Rev. **D25** (1982) 2649.
- [30] P. Hasenfratz, V. Laliena and F. Niedermayer, hep-lat/9801021; P. Hasenfratz, hep-lat/9702007.
- [31] U. Heller, K. Bitar, R. Edwards, A. Kennedy, Phys. Lett. 335B, 71 (1994).

[32] R. Sommer, Nucl. Phys. B411 (1994) 839.

[33] G. Boyd, et. al., Phys. Rev. Lett. **75** (1995) 4169.